A MAGYAR
TUDOMÁNYOS AKADÉMIA
CSILLAGVIZSGÁLÓ
INTÉZETÉNEK
KÖZLEMÉNYEI

MITTEILUNGEN
DER
STERNWARTE
DER UNGARISCHEN AKADEMIE
DER WISSENSCHAFTEN

BUDAPEST-SZABADSÁGHEGY

Nr. 68.

L. G. BALÁZS

DISTRIBUTION OF STARS OF SPECTRAL TYPES F7 AND EARLIER IN A LYRA REGION

BUDAPEST, 1975

DISTRIBUTION OF STARS OF SPECTRAL TYPES F7 AND EARLIER IN A LYRA REGION

SUMMARY

A study has been made of the spatial distribution of early type stars in a region of intermediate galactic latitude. Objective prism plates were used to survey an area of 19.5 □° in Lyra for all stars of spectral type F7 and earlier down to 13th photographic magnitude. 524 stars were detected, for which spectral types and photographic UBV colours were obtained. The stars were separated into four groups - spectral class A1 and earlier, A2-A7, A8-F2, and F3-F7 - and the space densities determined for each group. The space density curves show that the first two groups both appear to be composed of two kinematically distinct subsystems, each having a Gaussian velocity distribution but with a ratio of the velocity dispersions of 1.8:1. These two subsystems probably differ in age and it may be significant that the derived age difference, about 3×10^8 years, is close to the time-difference between two consecutive periods of star formation predicted by the density wave theory of spiral structure. Further observations, however, are needed to rule out other birth mechanisms having the same characteristic time.

INTRODUCTION

The distribution of the stars off the galactic plane is of considerable interest in order to understand some of the dynamical properties of our stellar system. To derive the three-dimensional distribution, we must analyse data concerning the apparent surface distribution in those galactic latitudes that are usually called "high" ($|b|$ approx. $\geq 40^{\circ}$) and "intermediate" (approx. $40^{\circ} \gtrsim |b| \geq 10^{\circ}$). The overwhelming majority of objects recognisable in high and intermediate galactic latitudes belongs to mean main-sequence stars and ordinary giants of spectral types A - K. In this paper we analyse stars F7 and earlier in an area of 19.5 □° in Lyra.

OBSERVATIONAL MATERIAL

An area of 19.5 square degrees centred on $l = 62.69^\circ$, $b = +15.99^\circ$ ($\alpha = 18^h42^m$, $\delta = +33^\circ20'$) was chosen for investigation. The observations were carried out with the 60/90/180 cm Schmidt telescope of the mountain station of the Konkoly Observatory. Spectral types and UBV colours were derived for 524 stars brighter than 13th photographic magnitude. The spectral classes are based on three objective prism plates taken with a 5° UBK7 (uv transmitting) prism that gives a dispersion of 580 Å/mm at Hγ. Kodak OaO emulsions were used, and the widening was 18", equivalent to 0.16 mm on the plate. The classification criteria were those given by STOCK and SLETTEBAK (1959) and STOCK (1971). The plates were made with double exposures of 6^m and 24^m so that any systematic variations in the classification with photographic density could be estimated.

The UBV photometry is based on four plates taken in each colour. The filters, emulsion types, and exposure times used are given in the following table:

U:	Kodak OaO + Schott UG1 2 mm filter	exp. time: 10^m
B:	Kodak OaO + Schott GG13 2 mm filter	" " : 5^m
V:	Kodak OaD + Schott GG14 2 mm filter	" " : 4^m

The international system is connected with the instrumental system according to the equations:

$$V_{instr} = V - 0.05(B-V) - 0.01$$
$$(B-V)_{instr} = 1.08(B-V) + 0.04$$
$$(U-B)_{instr} = 1.11(U-B) - 0.04(B-V) + 0.02$$

The plates were measured with the Becker-type iris photometer of the Konkoly Observatory, using a photoelectric sequence obtained with the Konkoly Observatory 60 cm photometric telescope. The mean errors of the photographically determined colours are $\pm 0\overset{m}{.}08$, $0\overset{m}{.}07$ and $0\overset{m}{.}06$ for U, B, and V, respectively.

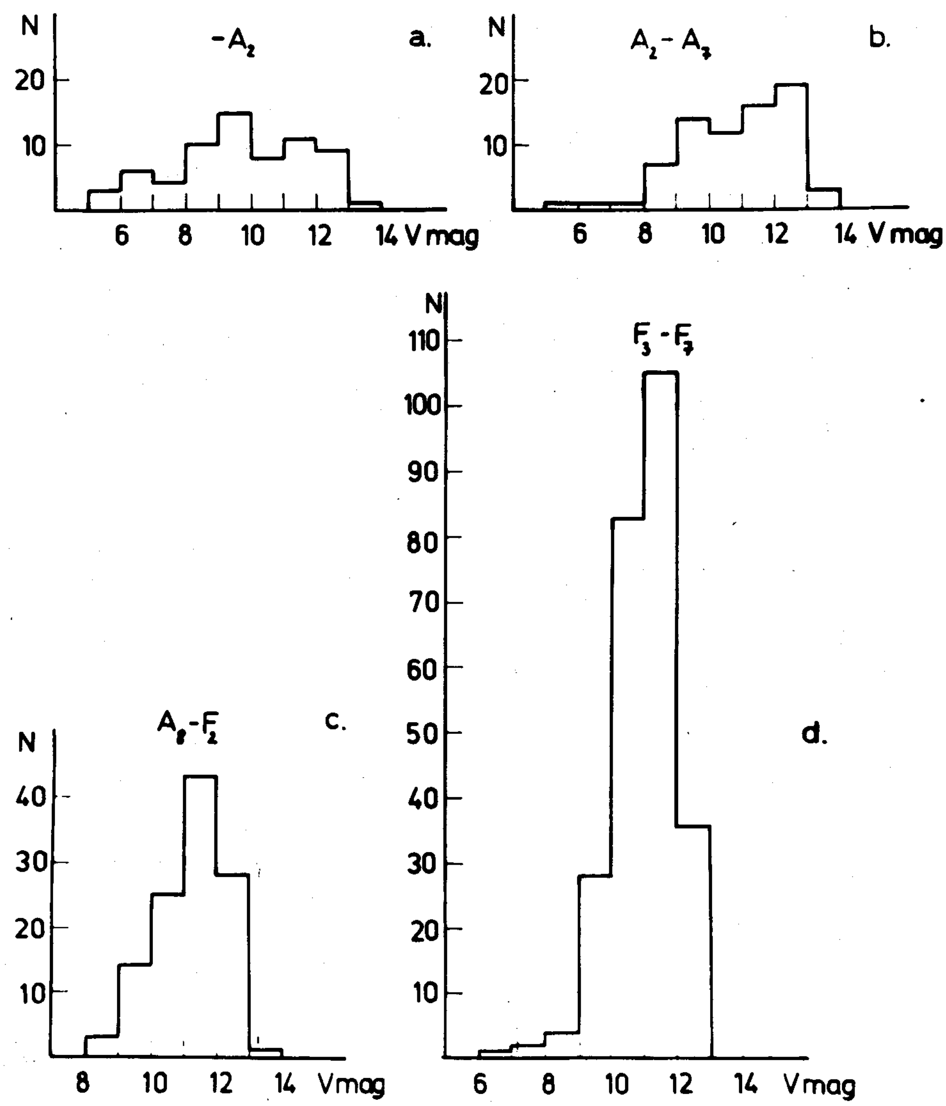

Figure 1.a.-d. The distribution of the stars against V magnitude.

THE SPACE DISTRIBUTION OF THE STARS

According to the sharpness of the classificational criteria and to the number of stars in each subclass four subgroups were determined: Stars earlier than A2, A2-A7, A8-F2, and F3-F7. The distribution of the stars against the V magnitude, in the subgroups defined, are demonstrated in Figs. 1a-1d. For determining the interstellar absorption the stars in each subgroup were divided into five groups according to their visual brightness: <7; 7-9; 9-11; 11-12; and >12. For each subgroup mean spectral types and colour indices were determined. Adopting JOHNSON's (1963) relation between intrinsic colour indices and spectral types the E_{B-V} and E_{U-B} colour excesses were obtained. The colour excesses determined by this method are plotted in Fig. 2. as a function of the distance modulus obtained by substracting from the mean V magnitude of each subgroup the absolute magnitude belonging to the mean spectral type. Adopting a ratio of total to selective absorption $R = A_V/E_{B-V} = 3$ for the total absorption a value $A_V = 0.06\rho$ could be obtained, where $\rho = V-M_V$. According to this formula the absorption in the observed direction at a distance of 300 pc amounts to 75% of the absorption at 1000 pc indicating that the interstellar dust is concentrated in a 80 pc half thick layer along the galactic plane for this galactic longitude. Our determination is in good agreement with FITZGERALD's (1968) data ($0.1 \leq E_Y < 0.2$) for this area.

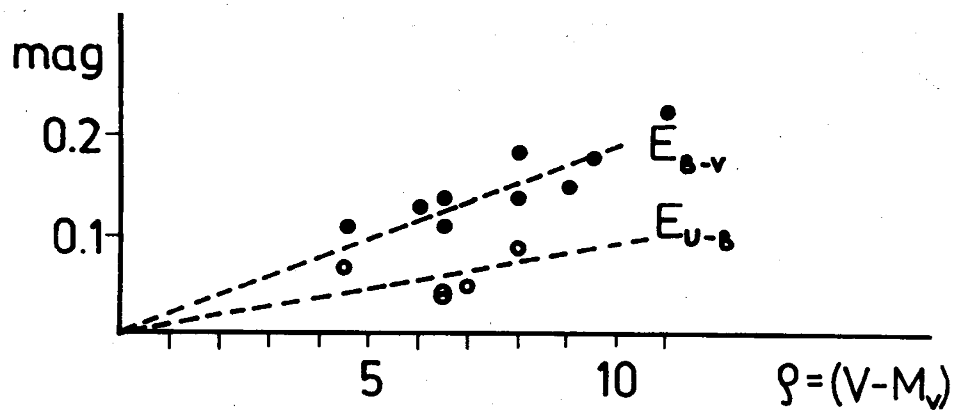

Figure 2. The colour excesses (E_{B-V} and E_{U-B}) as functions of uncorrected distance modulus.

The space densities were derived by grouping the stars in order of the distance modulus, obtained from the measured V magnitude and the mean absolute magnitude of the spectral type, corrected for the absorption and dividing the number of stars by the volume containing them. Assuming a Gaussian distribution of absolute magnitudes at a given spectral type the mean absolute magnitude at a given visual brightness can be obtained using the basic convolution equation of stellar statistics. The computation results the formula (MALMQUIST 1936)

$$\overline{M(m)} = M_o - \frac{\sigma^2}{A(m)} \frac{dA(m)}{dm}$$

where M_o, σ, and $A(m)$ are the intrinsic absolute magnitude, the standard deviation of the Gaussian distribution, and the number of stars in a $m \pm \frac{1}{2}$ interval, respectively.

The densities derived by this method are plotted in Figs. 3a-3d. The dashed lines show the limit of the completness of the sample caused by the limiting magnitude of classification. We shall discuss in the following section the spatial-distribution of the stars of each subclass separately and in more detail.

DISCUSSION OF THE SPACE DENSITIES

The density-gradients ($\frac{\partial \nu}{\partial r}$) of the different subgroups are nearly the same up to 600 pc, except for the break-down caused by the plate limit. At about 600pc the density-gradient of the A2-A7 stars changes and becomes smaller. A similar change is visible in the distribution of stars younger than A2 at 1000 pc but it is based on a small number of stars and therefore its singificance is questionable. Other authors (VAN RHIJN 1955, KUROCHKIN 1958, PERRY 1969, WOLLEY and STEWARD 1967), however, derived a similar change in the density gradient at stars younger than A2 so this effect in our case seems to be realistic. The spatial distribution of the A stars near the galactic poles shows a similar space density curve as those stars in our case. The similarity between this distributions and those obtained by the present investigation suggests that the observed density gradients of stars younger than A2, and A2-A7, in our case, are mainly due to the contributions of the gradients perpendicular to the galactic plane to the gradient in the line of sight.

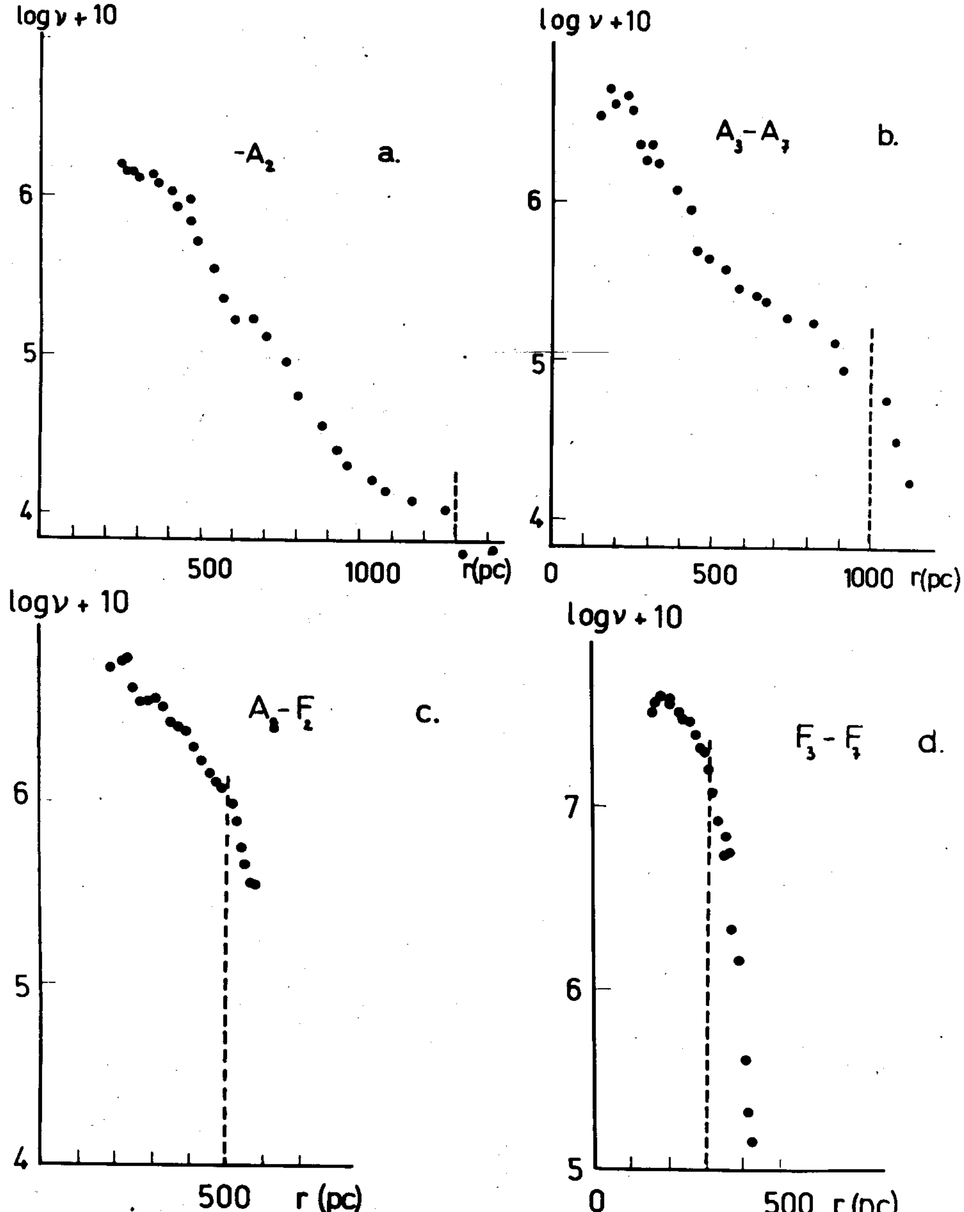

Figure 3.a.-d. The derived space densities of the different subgroups. (The dashed lines show the limit of the completness of the sample.)

Supposing that the distribution of stars in the phase space is an even function of the Z velocity component we can derive the following relation connecting the spatial density, the standard deviation of the Z velocity component and the gravitational potential (OGORODNIKOV 1965):

$$\frac{\partial(\nu\sigma_z^2)}{\partial z} = -\nu\frac{\partial\Phi}{\partial z}$$

After integration and elementary computations we obtain:

$$\sigma_z^2(z) = -\frac{\nu(0)}{\nu(z)}\left\{\int_0^z \frac{\partial\Phi}{\partial z}\frac{\nu(z)}{\nu(0)}\,dz - \sigma_z^2(0)\right\}$$

In our case we can take ν from our observations making the assumption that ν depends mainly on the z coordinate. We assume that the same holds for $\frac{\partial\Phi}{\partial z}$ in the direction observed and take it from the observations in the galactic caps (reviewed by OORT 1965). $\sigma_z(0)$ may be varied inside reasonable limits according to the observed data. If the formula given above has resulted a horizontal straight line in the $\sigma_z(z);z$ diagram we should assume that the velocity distribution, in the area observed, is Gaussian, since in that case $\sigma_z(z)$ is independent of z. Using the eye-estimated density curve of the stars A2-A7 derived from our observations and substituting $\sigma_z(0)=6.8$ km/sec we get the curve plotted in Fig.4. The curve runs approximately horizontally up to 70pc and above 180 pc, and the ratio of the velocity dispersions characterising the two horizontal parts of the curve equals to 1:1.8. Nearly the same ratio (1:2) was observed by WOOLLEY et al. (1969) and HARDING et al. (1971) for A0 stars in the south galactic cap. For $\sigma_z(0)$ they obtained 9 km/sec. Therefore the shape of the density curve may be explained as a superposition of two Gaussian velocity distributions having the above ratio of the velocity dispersions. At z = 0 the ratio of the densities of the two subsystems equals to about 1:7, and 1:70 in the case of stars younger than A2 if we adopt the change of the density gradient at r = 1000 pc as a real effect. It is to be mentioned that JONES (1972) found that the M giants in the south galactic cap had a similar dispersion dependence to those plotted in Fig.4. His $\sigma_z(0)=7$ km/sec agrees very well with our value but the increase of velocity dipersion is stronger than in our case.

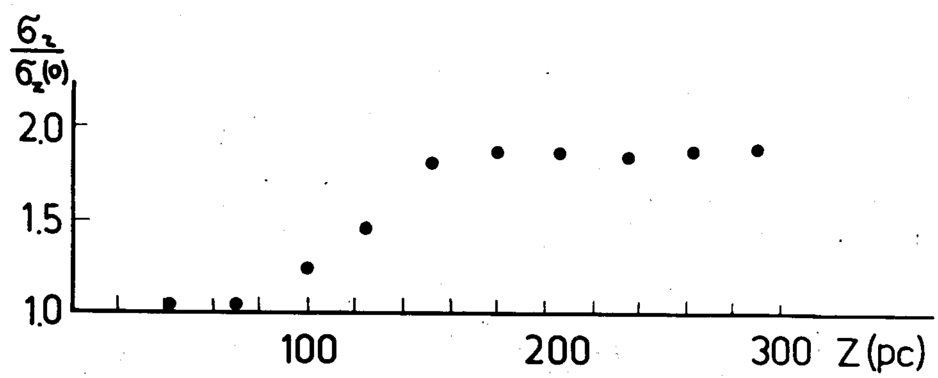

Figure 4. The $\sigma_z(z)/\sigma_z(0)$ ratio computed from the density curve of A2-A7 stars plotted against the height (z) above the galactic plane.

The explanation that the shape of the density curve and the z dependence of the velocity dispersion of the A type stars caused by a condensation of those stars around the sun seems to be improbable, because the search for determining the spatial density of these stars, reported by McCUSKEY (1965), does not show significant condensation in the direction of our observed area projected onto the galactic plane. Moreover the condensations are different at different spectral types but in our case the density gradients are nearly independent of the spectral type at the first part of the density curves.

The less compact subsystem is more prominent among the A2-A7 stars than among stars earlier than A2, which have mostly a spectral type B8 or later. Fig. 5 shows the logarithmic ratio of the density of the less compact component to the total density at z=0 using the data of different investigators. The most prominent feature in this figure is the "break" at A0 in the values of the ratios.

If stars are born continuously the exsistence of two kinematically different subsystems would be difficult to explain. This supports the idea of steplike birth. Taking into account that the

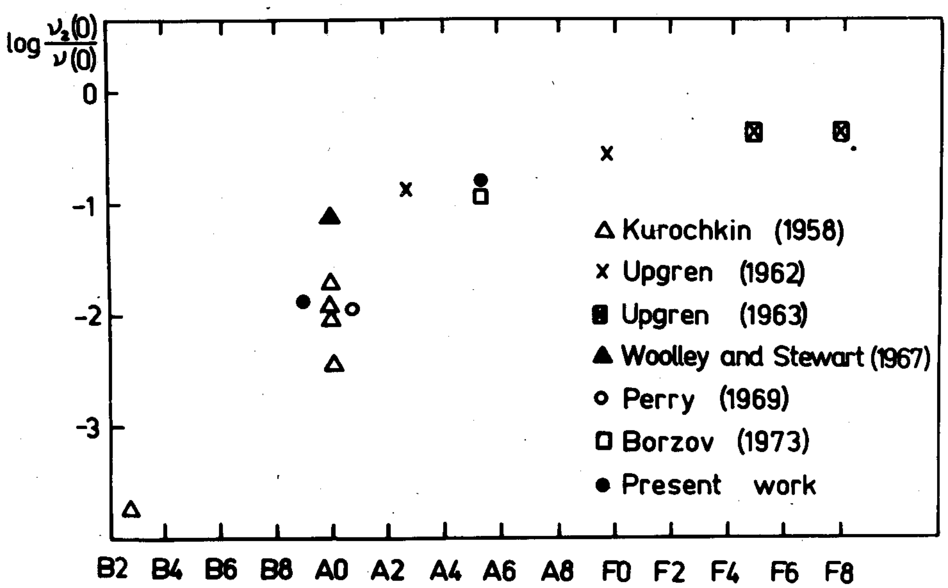

Figure 5. The logarithm of the ratio of the density of the less compact component to the total density at z=0 using the data of different investigators.

young stars are more concentrated to the galactic plane than the older stars and that the less compact subsystem increases in its prominence towards stars having longer lifetimes it is reasonable to suppose that the two kinematically different subsystems differ in age,too. The time difference between two "birth events" may be estimated by the lifetime of the stars at which the "break" appears in Fig. 5. Using the theoretical lifetimes published by IBEN (1967) and the empirical bolometric absolute magnitudes of DAVIS and WEBB (1970) and the absolute visual magnitudes of JUNG (1970, 1971) the lifetimes of the A0 stars are about 3×10^8 years. The uncertainties of the spectral classification of the late type B and early type A stars on spectrograms of small scale determine a confidence interval around A0 in Fig. 5. The edges of this interval are the spectral types B8 and A2. The lifetime τ of the stars at which the "break" appears lies therefore in the interval: 1.5×10^8 yrs$<\tau<5.5\times10^8$ yrs. According to the density wave theory (LIN and SHU 1964, 1966, LIN et al. 1969) a stream of stars and interstellar matter passes the density wave twice in a rotational period generating a shock wave in the interstellar matter (ROBERTS 1969) which causes a high stellar birth rate. The time between two passages equals to 2.5×10^8 years at the distance of the sun from the galactic centre. Our estimated time of 3×10^8 years is close to this theoretical value within the uncertainties of the estimation.

According to this picture the newly formed stars in the shock front of the density wave would have nearly circular orbits and a small velocity dispersion. As WOOLLEY and CANDY (1968) pointed out the interaction between the irregularities of the galactic gravitational field and the stars having small eccentricity orbits causes an increase of the eccentricity and, consequently, of the velocity dispersion perpendicular to the galactic plane. Therefore the older subsystem has a greater dispersion.

On the basis of the present observational material it is not possible to rule out other birth mechanisms having the same characteristic time. However, in directions in which the distances to the shock front along the stream lines and consequently the time passed are different we may expect differences in the changes of the velocity dispersions and of the spatial densities perpendicular to the galactic plane.

CONCLUSIONS

The shape of the space density curve of the B8-A1 and A2-A7 type stars may be explained as a superposition of two Gaussian velocity distributions having a ratio of the velocity dispersions of 1:1.8. The existence of two kinematically different subsystems supports the idea of steplike formation of the stars. The time difference between two "birth events", about 3×10^8 years, is close to the time the star streaming needs between two passages of the density wave. On the basis of the present observational material it is not possible to rule out other birth mechanisms having the same characteristic time. Observations in directions in which the distances to the shock front along the stream lines are different may solve the problem.

ACKNOWLEDGEMENTS

I am indebted to Dr. B.A. Balázs, for calling my attention to this problem and to Dr. B. Szeidl for the photoelectric observations and to both of them for valuable discussions. I am grateful to Mrs. B. Kálmán and Mrs. Zs. Litvay for their assistance in analysing the data.

REFERENCES

Borzov, G.G., 1973, AZh. 50. 1041

Davis, J. and Webb, R.J. 1970, ApJ. 159. 551

FritzGerald, M.P. 1968, AJ. 73. 983

Harding, G.A., Fakim, F. and Haslam, M.C. 1971, Royal Obs. Bull. No.165

Iben, I.I., 1967, Ann. Rev. of Astron. and Astrophys. 5, 571

Johnson, H.L., 1963, Photometric Systems in 'Basic Astronomical Data', Ed.K.Aa.Strand, Univ. Chicago Press, Chicago, p.204.

Jones, D.H.P., 1972, ApJ. 178. 467

Jung, J., 1970, Astron. Astrophys. 4. 53

Jung, J., 1971, Astron. Astrophys. 11. 351

Kurochkin, N.E., 1958, AZh. 35. 86

Lin, C.C., and Shu, F.M., 1964, ApJ. 140. 646

Lin, C.C., and Shu, F.M., 1966, Proc.Nat. Acad.Sci. USA 55. 229

Lin, C.C., Yuan, C., and Shu, F.M., 1969, ApJ. 155. 721

Malmquist, K.G., 1936, Stockholms Obs.Medd., No.26

McCuskey, S.W. 1965, Distribution of Stars in the Galactic Plane in 'Galactic Structure', Ed. A.Blauw and M. Schmidt, Univ. Chicago Press, p.1.

Ogorodnikov, K.F. 1965, Dynamics of Stellar Systems, Pergamon Press, p.255

Oort, J.H. 1965, Stellar Dynamics in 'Galactic Structure', Ed. A.Blauw and M.Schmidt, Univ.Chicago Press p.455

Perry, C.L. 1969, AJ. 74. 139

Roberts, W.W., 1969, ApJ. 158. 123

Slettebak, A. and Stock, J., 1959, Astr.Abhandlungen der Hamburger Sternwarte Bd.V. Nr.5

Stock, J., 1971, Application of Objective Prism Techniques in the Magellanic Clouds in 'The Magellanic Clouds,' Ed. A.B.Muller, D. Reidel Publishing Co., p.181

Upgren, A.R., 1962, AJ. 67. 37

Upgren, A.R., 1963, AJ. 68. 194

Van Rhijn, P.J. 1955, Publs. Kapteyn Astr.Lab. Groningen, No.57

Woolley, R. and Steward, J.M. 1967, MN. 136. 329

Woolley, R. and Candy, M.P. 1968, MN. 139, 231

Woolley, R., Asaad, A.S., Candy, M.P., and Penston, M.J. 1969, Royal Obs. Bull. No. 156

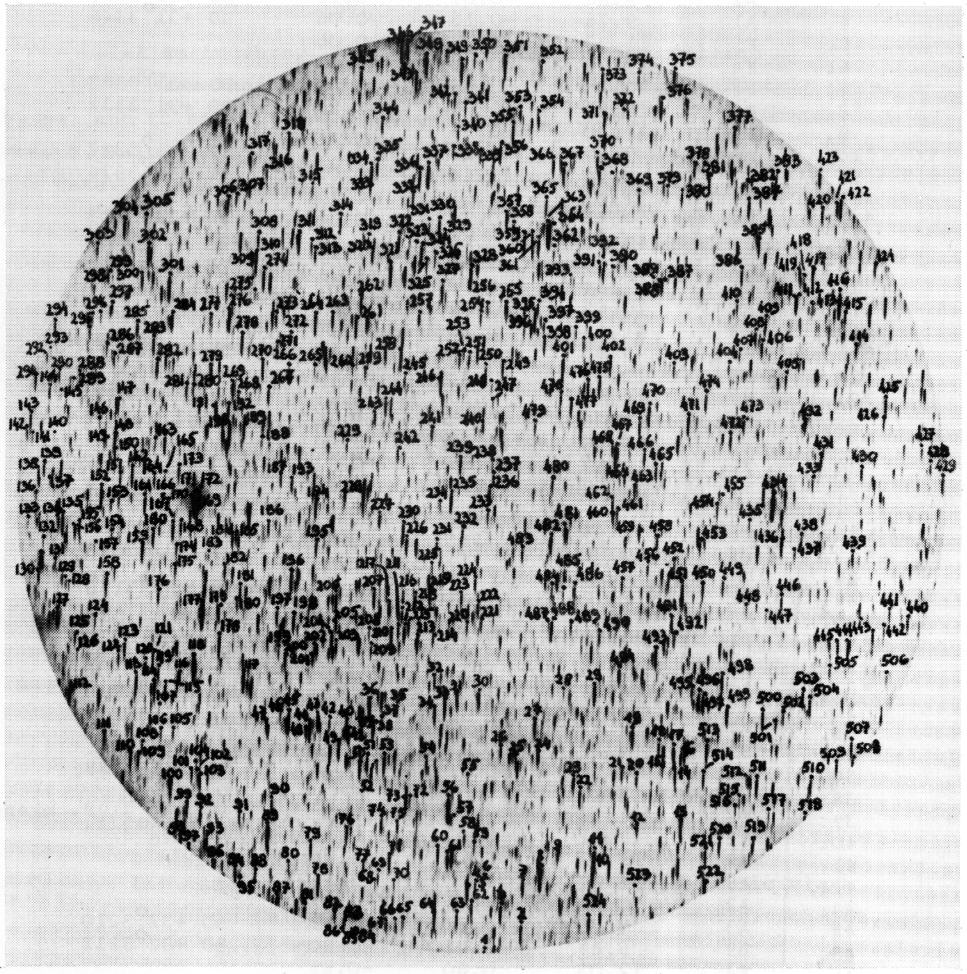

Finding chart of the survey stars. North is at the top and East is at the left.

TABLE

Spectra and UBV data of the survey stars

No.	Sp.	V	B-V	U-B	remarks
1.	A1	10.86	-0.19	0.01	BD +31°3341
2.	F5	9.97	0.39	-0.05	BD +31°3334
3.	A2	9.86	-0.07	0.15	BD +31°3338
4.	A1	9.76	-0.15	0.06	BD +31°3346
5.	F5	11.92	0.19	0.06	
6.	F4	12.32	0.38	-0.05	
7.	F7	10.18	0.45	0.02	BD +31°3333
*8.	A1	6.39	-0.04	-0.26	BD +31°3332
9.	F5	11.30	0.56	-0.03	
*10.	A2	7.37	0.28	0.05	BD +31°3327
11.	F7	9.94	0.44	-0.02	BD +31°3326
12.	F6	11.45	0.51	-0.12	
*13.	A3	9.17	0.16	0.05	BD +31°3317
14.	F5	10.50	0.49	-0.07	
15.	F5	12.09	0.54	-0.06	
16.	A2	11.84	0.27	0.18	
17.	F6	10.67	0.32	0.07	
18.	A3	11.69	0.20	0.06	
*19.	A1	9.88	0.30	0.03	BD +32°3177
20.	F2	12.03	0.43	-0.08	
*21.	A7	11.50	0.39	0.07	
22.	B2	11.36	-0.14	0.16	
*23.	F0	10.70	0.29	0.04	
24.	F5	10.67	0.57	-0.11	BD +32°3184
*25.	F5	11.59	0.65	-0.11	
26.	F5	11.44	0.52	-0.07	
*27.	F2	10.36	0.37	0.00	BD +32°3186
28.	F4	12.84	0.85	-	
29.	A9	9.78	0.34	-0.07	BD +32°3178
*30.	F3	11.04	0.35	-0.05	
*31.	F1	10.80	0.27	-0.03	
*32.	A7	11.65	0.27	0.01	BD +32°3199
*33.	F2	10.34	0.53	0.05	
34.	F7	10.26	0.60	-0.09	BD +32°3191
35.	A7	11.91	0.20	0.02	
36.	B9	9.22	-0.06	-0.08	
37.	F3	12.35	0.46	-0.20	BD +32°3199
38.	F5	12.10	-	-	blend
39.	F7	9.10	-	-	BD +32°3198, blend
40.	A2	8.91	-0.01	0.10	BD +32°3203
41.	A3	11.43	0.11	-0.09	
42.	A6	11.99	0.40	-0.14	
43.	A2	10.83	0.36	-0.01	
44.	A3	8.55	0.30	0.13	BD +32°3210
45.	B9	8.89	-0.05	-0.20	BD +32°3212
46.	F4	12.03	0.50	-0.21	
47.	F2	11.38	0.38	-0.06	
48.	A7	11.54	0.48	-0.25	
49.	A8	9.30	0.16	-0.02	BD +32°3204
50.	F7	9.80	0.57	0.00	BD +31°3360

Table

/Continued/

No.	SP.	V	B-V	U-B	remarks
51.	F6	9.92	0.69	0.18	
52.	A5	12.64	0.49	-0.26	
53.	A9	10.30	0.29	-0.07	BD +31°3358
54.	F6	10.91	0.57	-0.20	
*55.	A3	12.79	0.33	-0.02	
*56.	A9	5.68	0.35	0.00	BD +31°3348
57.	A7	12.59	0.36	-0.22	
58.	A7	11.81	0.24	-0.16	
59.	A4	12.41	0.16	-0.13	
60.	F6	10.04	0.42	-0.06	BD +31°3349
61.	F5	10.47	0.35	-0.15	
62.	A5	10.91	0.28	-0.07	
63.	F5	10.68	0.37	-0.25	
64.	F6	9.31	0.40	-0.15	BD +31°3350
65.	F3	12.27	0.43	-0.06	
66.	F5	12.75	0.30	-0.27	
67.	A5	12.03	0.14	-0.07	
68.	A6	13.00	0.29	-0.22	
69.	F6	11.61	0.43	-0.20	
70.	A7	12.50	0.35	-0.16	
71.	A7	10.62	-0.17	-0.39	BD +31°3354
72.	F0	12.47	0.44	-0.25	
73.	F5	10.01	0.34	-0.02	BD +31°3352
74.	F5	11.45	0.53	-0.05	BD +31°3357
75.	F5	11.65	0.36	-0.14	
76.	F4	10.96	0.19	-0.01	
77.	F0	11.57	0.31	0.01	
78.	F0	9.27	0.26	0.03	BD +31°3362
79.	A7	10.21	0.08	0.09	BD +31°3363
80.	F0	11.75	0.25	-0.12	
81.	F5	10.62	0.37	0.01	
82.	F2	11.79	0.22	0.03	
83.	F5	11.82	0.33	-0.15	
84.	A9	11.02	0.14	0.19	
85.	F2	12.54	0.43	-0.05	
86.	F4	11.50	0.18	-0.02	
87.	A6	9.58	0.09	0.10	BD +31°3368
88.	F5	11.08	0.40	-0.07	
*89.	B4	6.04	-0.14	-0.61	BD +31°3369
90.	F1	11.42	0.25	-0.09	
91.	A5	11.88	0.21	0.00	
92.	A0	10.86	0.00	0.03	BD +31°3372
93.	F0	10.89	0.14	-0.02	
94.	F2	11.87	0.36	-0.27	
95.	F2	11.28	0.26	-0.10	
96.	A0	8.48	-0.05	-0.09	BD +31°3371
*97.	B6	6.62	-0.01	-0.11	BD +31°3373
98.	A2	9.44	-0.08	0.05	BD +31°3374
99.	F1	10.95	0.28	-0.06	
100.	F5	10.56	0.47	-0.06	

Table
/Continued/

No.	Sp	V	B-V	U-B	remarks
101.	F2	11.28	0.31	0.05	
102.	F6	12.21	0.86	-0.20	
103.	F4	10.62	0.36	-0.02	
104.	F0	12.43	0.44	-0.32	
105.	F6	11.8	-	-	blend
106.	F4	12.24	0.45	-0.27	
107.	A9	13.03	0.52	-0.10	
108.	F1	12.01	0.34	-0.10	
109.	F1	11.53	0.28	-0.19	
110.	A9	10.71	0.07	0.16	BD +31°3379
111.	F7	10.81	0.76	0.24	
112.	F5	9.82	0.37	0.08	BD +32°3238
113.	F4	9.87	0.30	0.06	BD +32°3233
114.	B9	9.83	-0.05	0.17	BD +32°3230
115.	A7	10.58	0.19	0.04	BD +32°3229
116.	F5	11.0	-	-	
117.	A3	8.56	0.14	0.10	BD +32°3221
*118.	A3	5.22	0.11	0.03	BD +32°3228
119.	F5	11.10	0.56	-0.13	
120.	A9	11.62	0.24	-0.09	
121.	F5	10.64	0.40	0.01	
122.	F4	11.50	0.47	-0.19	
123.	F3	10.14	0.34	0.09	BD +32°3235
124.	F5	12.14	0.42	-0.14	
125.	F4	11.96	0.50	-0.19	
126.	F2	12.75	0.59	-0.07	
127.	A2	9.70	-0.01	0.19	BD +32°3242
128.	F6	12.41	0.57	-0.18	
129.	F5	12.29	0.57	-0.30	
130.	F5	11.31	0.34	-0.02	
131.	A4	12.34	0.29	-0.06	
132.	F3	12.39	0.85	-0.10	
133.	F4	12.46	0.58	-0.21	
134.	F4	11.20	0.36	0.04	
135.	A0	8.83	0.03	0.26	BD +33°3245
136.	F4	12.21	0.61	-0.18	
137.	F5	12.54	0.73	-0.23	
138.	F3	10.94	0.26	0.11	
139.	F5	11.02	0.37	-0.03	
140.	F3	12.83	0.64	-	
141.	F5	12.44	0.54	-0.21	
142.	A5	11.87	0.25	0.01	
143.	A5	10.50	0.11	0.18	
144.	F5	11.15	0.54	-0.04	
145.	A3	12.83	0.61	-	
146.	A	12.92	0.76	-	
147.	F2	11.01	0.48	0.13	BD +33°3239
148.	F2	10.39	0.36	0.08	BD +33°3238
149.	F4	12.46	0.57	-0.24	
150.	A4	12.07	0.37	-0.07	

Table
/Continued/

No.	Sp.	V	B-V	U-B	remarks
151.	F2	11.8	-	-	blend
152.	B8	8.65	0.08	0.04	BD +33°3241
153.	F6	12.38	0.62	-0.18	
154.	A8	12.24	0.41	0.05	
155.	F1	10.74	0.35	0.14	BD +33°3244
156.	F6	10.99	0.42	0.03	
157.	A6	12.72	0.51	-0.21	
158.	A1	11.63	0.03	-0.10	
159.	F3	9.89	0.54	0.10	BD +32°3234
160.	F1	10.17	0.29	0.14	BD +32°3232
161.	A4	9.75	0.14	0.33	BD +33°3232
162.	F2	9.09	0.51	-0.01	BD +33°3236
163.	A8	12.17	0.57	-0.16	
164.	A6	11.69	0.30	0.03	
165.	F3	12.43	0.58	-0.19	
166.	F0	12.15	0.51	-0.09	
167.	F6	10.8	-	-	BD +33°3228 blend
168.	F4	11.03	0.47	0.07	
169.	F3	10.1	-	-	blend
170.	B2	7.0	-	-	blend
171.	A1				BD +33°3223, β Lyrae
172.	A7	9.79	0.23	0.43	
173.	A9	10.97	0.65	0.08	
174.	F6	11.44	0.56	-0.02	
175.	F1	11.58	0.59	0.00	
176.	A2	11.38	0.31	0.19	
*177.	B2	5.89	-0.16	-0.65	BD +32°3227
178.	F6	8.66	0.56	0.10	BD +32°3223
179.	A8	10.86	0.29	0.23	
180.	F5	11.98	0.59	-0.19	
181.	F3	11.01	0.51	-0.03	
182.	F6	10.67	0.41	0.37	
183.	F6	11.77	0.59	-0.16	
184.	F5	11.11	0.46	0.09	
185.	F3	11.92	0.43	0.07	
186.	F5	11.16	0.50	-0.01	
187.	F0	11.42	0.64	0.06	
188.	F0	12.50	0.61	-	
189.	F2	10.24	0.44	0.06	
190.	A2	6.84	0.37	0.09	BD +33°3215
191.	F7	10.61	0.52	0.14	BD +33°3219
192.	F0	10.44	0.35	0.18	
193.	F0	11.6	-	-	blend
194.	F5	9.9	-	-	BD +33°3204, blend
195.	F3	11.08	0.45	0.01	
196.	A5	9.00	0.19	0.25	BD +32°3214
197.	F4	10.93	0.45	0.05	
198.	F2	10.12	0.43	0.00	
199.	F4	12.19	0.64	-0.28	
200.	F2	10.80	0.37	0.03	

Table

/Continued/

No.	Sp.	V	B-V	U-B	remarks
201.	FO	11.48	0.48	-0.03	
202.	F6	11.92	0.58	-0.19	
203.	F6	11.41	0.55	-0.19	
204.	F6	10.28	0.51	0.04	BD $+32^{O}3208$
205.	A5	11.98	0.13	0.16	
206.	F5	10.01	0.40	0.09	BD $+32^{O}3207$
207.	F2	9.89	0.38	0.18	BD $+32^{O}3200$
208.	F5	12.06	0.65	-0.28	
209.	F5	11.67	0.59	-0.15	
210.	A4	9.77	0.19	0.15	BD $+32^{O}3195$
211.	F3	11.54	0.52	-0.19	
212.	F2	10.13	0.40	0.00	
213.	F6	10.43	0.56	-0.03	BD $+32^{O}3194$
214.	FO	12.27	0.42	-0.04	
215.	F5	10.54	0.58	0.00	
216.	F2	11.62	0.50	-0.10	
217.	F1	11.18	0.16	0.02	
218.	F2	10.68	0.43	0.02	
219.	A1	9.76	0.13	0.16	BD $+32^{O}3193$
220.	A7	11.23	0.44	0.19	
221.	A3	11.76	0.27	0.13	
222.	F5	10.97	0.58	0.03	
223.	F1	10.77	0.66	0.15	
224.	F5	10.90	0.49	-0.02	
225.	F6	12.25	0.61	-0.19	
226.	A6	10.21	0.13	0.19	BD $+33^{O}3193$
227.	FO	11.01	0.27	0.09	BD $+33^{O}3196$
228.	A4	9.57	0.19	0.17	BD $+33^{O}3200$
229.	F6	11.87	0.75	-0.22	
230.	F6	9.35	0.47	-0.06	BD $+33^{O}3194$
231.	F5	11.03	0.40	0.15	
232.	B9	11.62	0.07	0.07	
233.	F5	11.92	0.17	0.02	
234.	A3	12.70	0.30	-0.16	
235.	A5	8.99	0.21	0.20	BD $+33^{O}3188$
236.	F4	11.08	0.38	0.09	
237.	FO	11.48	0.40	-0.03	
238.	F3	12.49	0.61	-0.28	
239.	F4	9.71	0.48	0.19	BD $+33^{O}3187$
240.	A3	11.5	-	-	
241.	FO	11.33	0.27	0.17	
242.	F5	11.14	0.58	-0.26	
243.	F5	11.04	0.51	-0.17	
244.	F6	10.29	0.47	0.14	
245.	F5	11.97	0.45	-0.26	
246.	F7	7.56	0.83	0.14	BD $+33^{O}3190$
247.	F5	11.3	-	-	
248.	A9	12.23	0.61	-0.08	
249.	F5	10.15	0.69	0.16	BD $+33^{O}3185$
250.	F5	11.57	0.58	0.05	

Table
/Continued/

No.	Sp.	V	B-V	U-B	remarks
251.	F5	11.63	0.61	0.11	BD +33°3186
252.	F4	11.44	0.70	-0.06	
253.	AO	12.50	0.32	-0.23	
254.	F6	11.13	0.70	0.06	
255.	F6	10.69	0.73	0.08	
256.	F6	11.42	0.91	-0.05	
257.	A7	10.33	1.56	1.28	
258.	AO	9.45	0.10	0.20	BD +33°3195
259.	F6	11.90	0.68	-0.18	
260.	A1	12.43	0.40	-0.02	
261.	F6	9.59	0.55	0.18	BD +34°3313
262.	F6	9.52	0.61	0.13	BD +34°3314
263.	F1	10.34	0.36	0.10	
264.	F7	8.17	0.57	0.06	BD +34°3317
265.	FO	12.25	0.53	-0.21	
266.	F5	12.19	0.53	-0.24	
267.	FO	10.35	0.30	0.19	BD +33°3210
268.	F4	11.52	0.40	0.08	
269.	B5	11.25	-0.04	-0.38	
270.	F6	8.78	0.54	0.10	BD +33°3212
271.	F1	11.85	0.45	0.05	
272.	A8	12.36	0.41	-0.11	
273.	F5	10.78	0.65	0.09	
274.	A4	8.81	0.29	0.21	BD +34°3325
275.	F5	12.46	0.58	-0.17	
276.	AO	7.82	0.25	0.26	BD 34°3729
277.	F4	11.89	0.36	0.07	
278.	F7	8.35	0.58	0.20	BD +33°3214
279.	F5	10.18	0.44	0.14	BD +33°3221
280.	F6	11.59	0.55	-	
281.	F3	11.19	0.44	-0.06	
282.	F6	10.00	0.44	0.17	BD +33°3231
283.	A4	10.10	0.13	0.24	BD +33°3233
284.	A3	9.55	0.36	0.30	BD +34°3333
285.	F2	10.89	0.33	0.09	BD +34°3338
286.	F5	12.09	0.51	-0.11	
287.	F4	11.58	0.42	-0.06	
288.	F5	12.60	0.59	-0.19	
289.	F3	12.0	-	-	
290.	F5	11.60	0.49	0.04	
291.	F3	11.12	0.23	0.13	
292.	F6	11.76	0.76	-0.02	
293.	F5	12.52	0.68	-0.30	
294.	A3	11.53	0.29	0.12	
295.	F6	11.16	0.61	-0.15	
296.	F4	12.27	0.70	-0.36	
297.	F2	10.49	0.21	0.76	BD +34°3340
298.	A4	13.09	0.41	-0.31	
299.	AO	12.02	0.00	-0.16	
300.	A7	10.51	0.34	0.23	

Table
/Continued/

No.	Sp.	V	B-V	U-B	remarks
301.	A3	6.94	0.32	0.37	BD +34°3334
302.	A3	8.54	0.74	0.18	BD +34°3337
303.	F5	11.78	0.57	-0.20	
304.	F2	9.62	0.41	0.13	BD +34°3339
305.	A2	11.83	0.41	0.17	
306.	F4	10.91	0.59	-0.04	
307.	F4	11.84	0.61	-0.17	
308.	F2	10.96	0.52	0.01	
309.	A4	12.00	0.47	-0.03	
310.	F7	7.40	0.79	0.20	BD +34°3326
311.	B9	8.15	0.25	-0.01	BD +34°3319
312.	F4	11.44	0.66	-0.06	
313.	FO	11.10	0.43	0.11	
314.	F5	10.38	0.65	0.08	
315.	AO	11.68	0.27	-0.11	
316.	F5	11.66	0.65	-0.03	
317.	F5	11.40	0.67	-0.20	
318.	F2	9.70	0.47	0.24	BD +34°3321
319.	F6	11.94	0.80	-0.26	
320.	A1	11.14	0.39	0.10	
321.	A2	6.64	0.40	0.18	BD +34°3310
322.	F5	10.53	0.67	0.02	BD +34°3309
323.	AO	13.43	0.31	-	
324.	A8	9.19	0.49	0.16	BD +34°3303
325.	F6	11.21	0.65	0.03	
326.	F5	11.71	0.79	-0.19	
327.	F3	9.44	0.58	0.00	BD +34°3299
328.	A3	7.51	0.44	0.19	BD +34°3297
329.	F6	10.47	0.64	0.08	BD +34°3300
330.	A8	8.98	0.49	0.15	BD +34°3301
331.	B3	12.58	0.60	-0.20	
332.	F5	10.98	0.80	-0.01	
333.	F7	11.29	0.76	-0.08	
334.	A2	8.7	-	-	BD +34°3312,blend
335.	FO	10.51	0.61	0.18	
336.	A3	9.70	0.31	0.18	BD +34°3305
337.	B7	6.86	0.40	-0.18	BD +34°3302
338.	F5	11.21	0.75	-0.06	
339.	FO	11.58	0.50	-0.03	
340.	FO	11.97	0.73	-0.16	
341.	F3	11.58	0.74	-0.16	
342.	F5	11.29	0.77	-0.10	
343.	F4	10.42	0.63	0.07	
344.	A9	11.11	0.62	-	
345.	F6	10.14	0.76	0.11	BD +35°3359
346.	F2	9.45	0.51	0.13	BD +35°3353
347.	F1	11.31	0.72	-0.07	
348.	B9	9.13	0.42	0.11	BD +35°3349
349.	A7	8.76	0.36	0.22	BD +35°3346
350.	A2	12.17	0.36	-0.09	

Table

/Continued/

No.	Sp.	V	B-V	U-B	remarks
351.	F1	8.5	-	-	BD +35°3342, blend
352.	F4	11.80	0.74	-0.21	
353.	F1	11.31	0.61	0.00	
354.	F5	11.40	0.89	-0.26	
355.	B8	9.09	0.31	0.00	BD +35°3341
356.	F4	9.54	0.68	0.02	BD +34°3295
357.	A7	9.92	0.64	0.14	BD +34°3294
358.	A9	12.16	0.54	-0.08	
359.	A5	10.04	0.44	0.16	BD +34°3292
360.	F6	10.27	0.76	0.22	BD +34°3291
361.	A9	9.51	0.40	0.23	BD +34°3290
362.	F2	11.89	0.54	0.11	
363.	A0	7.8	-	-	blend
364.	B3	6.2	-	-	BD +34°3285, blend
365.	F6	10.70	0.69	0.10	
366.	A0	9.88	0.25	0.28	BD +35°3284
367.	A0	9.77	0.24	0.15	BD +34°3281
368.	F5	10.41	0.67	0.10	BD +34°3277
369.	F5	11.61	0.70	-0.15	
370.	F6	10.36	0.78	0.19	BD +34°3278
371.	F3	9.99	0.46	0.02	BD +35°3331
372.	A6	13.63	-	-	
373.	F5	9.84	0.69	0.10	BD +35°3333
374.	A2	12.16	0.41	-0.10	
375.	F4	-	-	-	on the edge of the plate
376.	A2	8.81	0.48	0.16	BD +35°3324
377.	F4	10.21	0.77	0.11	BD +35°3313
378.	A9	11.43	0.80	0.23	
379.	A5	12.33	0.59	0.01	
380.	F2	10.87	0.68	0.01	
381.	F5	10.45	0.87	0.13	BD +34°3268
382.	A9	12.54	0.50	0.09	
383.	F5	12.19	0.75	-	
384.	F4	9.19	0.73	0.11	BD +34°3263
385.	F5	10.03	0.63	0.15	BD +34°3261
386.	A7	10.35	0.56	0.15	
387.	A5	11.30	0.54	-0.12	BD +34°3272
388.	F0	11.3	-	-	blend
389.	F2	12.41	0.64	-0.23	
390.	A4	12.44	0.46	0.00	
391.	F5	11.26	0.63	-0.03	
392.	F6	10.03	0.72	0.16	BD +34°3276
393.	F4	12.36	0.66	-0.03	
394.	F5	10.94	0.62	0.05	
395.	A0	8.83	0.24	-0.05	BD +34°3289
396.	F6	10.41	0.65	0.29	
397.	F5	11.74	0.58	0.31	
398.	F2	9.86	0.59	0.12	BD +34°3283
399.	F2	11.78	0.72	-0.16	
400.	A9	11.40	0.54	0.11	

Table

/Continued/

No.	Sp.	V	B-V	U-B	remarks
401.	B4	7.20	0.11	-0.41	BD +33°3180
402.	F6	9.73	0.60	0.20	BD +33°3172
403.	A1	11.26	0.56	0.25	
404.	F5	11.66	0.60	0.05	
405.	F6	11.35	0.53	0.03	
406.	F5	10.49	0.63	0.12	
407.	A8	11.94	0.42	0.11	
408.	F5	10.86	0.56	0.12	BD +34°3260
409.	F5	10.97	0.55	0.05	
410.	F5	11.43	0.69	-0.01	
411.	B9	10.60	0.10	-0.07	BD +34°3252
412.	F5	11.16	0.62	0.11	
413.	F4	12.35	0.69	-0.19	
414.	F1	11.52	0.52	-0.02	
415.	F2	11.21	0.50	0.19	
416.	A0	5.80	-0.09	0.24	BD +34°3245
417.	A3	10.42	0.31	0.26	BD +34°3250
418.	F0	12.37	0.65	-0.02	
419.	A2	11.32	0.29	0.22	
420.	F5	10.59	0.75	-0.02	
421.	F1	11.56	0.52	0.06	
422.	A0	8.61	0.28	0.13	BD +34°3247
423.	F5	10.04	0.68	0.18	BD +34°3249
424.	A1	12.63	0.11	-0.46	
425.	A5	9.34	0.34	0.24	BD +33°3138
426.	A7	11.27	0.49	-0.01	
427.	F4	11.71	0.79	-0.19	
428.	F3	11.73	0.43	0.06	
429.	F3	10.20	0.35	0.21	
430.	A3	10.68	0.28	0.12	
431.	F5	10.92	0.64	-0.10	BD +33°3144
432.	F5	10.23	0.88	-0.06	BD +33°3149
433.	F5	11.20	0.70	-0.14	
*434.	A1	5.38	-0.10	-0.49	BD +33°3212
435.	F0	12.15	0.70	-0.20	
436.	A3	9.70	0.36	-0.01	BD +33°3152
437.	F4	11.91	0.63	-0.26	
438.	F5	11.85	0.67	-0.07	
439.	F5	10.73	0.59	0.00	
440.	F0	10.94	0.47	-0.03	
441.	F0	11.55	0.46	-0.01	
442.	A8	11.94	0.58	-0.13	
443.	F5	10.52	0.81	-0.12	
444.	A7	9.32	0.30	0.11	BD +32°3155
445.	A0	11.17	0.15	-0.12	
446.	F1	11.14	0.63	0.02	
447.	A5	12.41	0.78	-0.36	
448.	A6	12.25	0.51	-0.11	
449.	F6	10.69	0.69	0.03	
450.	F4	10.57	0.67	-0.10	

Table
/Continued/

No.	Sp.	V	B-V	U-B	remarks
451.	F7	9.30	0.76	-0.01	BD +32°3169
452.	F5	11.62	1.00	-0.27	
453.	F6	11.04	0.91	-0.20	
454.	F6	11.16	0.81	-0.28	
455.	A0	12.96	0.50	-	
456.	F5	11.80	0.66	-0.27	
457.	A5	11.54	0.58	-0.01	
458.	F6	11.54	0.60	-0.07	
459.	F5	10.15	0.70	-0.11	BD +32°3166
460.	F4	11.20	0.78	-0.20	
461.	F7	11.52	0.81	-0.19	
462.	F6	10.39	0.81	-0.17	BD +33°3169
463.	F5	11.78	0.68	-0.22	
464.	F3	11.57	0.68	-0.20	
465.	F5	10.56	0.70	-0.11	
466.	F6	10.67	0.69	-0.10	
467.	F6	6.90	0.83	0.08	BD +33°3171
468.	F0	11.47	0.64	-0.09	
469.	F3	9.84	0.64	0.07	BD +33°3167
470.	B8	8.51	0.40	-0.10	BD +33°3165
471.	F3	9.06	0.62	0.08	BD +33°3163
472.	F5	10.50	0.77	-0.17	
473.	F5	10.77	0.75	-0.03	
474.	F6	9.94	0.84	0.01	BD +33°3159
475.	B9	9.24	0.34	0.01	BD +33°3173
476.	F7	9.55	0.74	-0.05	BD +33°3174
477.	F5	9.53	0.86	0.01	BD +33°3179
478.	A2	10.99	0.44	0.12	
479.	A9	11.46	0.73	-0.14	
480.	F5	11.06	0.76	-0.14	
481.	A0	10.38	0.30	-0.01	BD +33°3178
482.	F7	9.51	0.90	0.30	BD +33°3181
483.	F6	10.92	0.75	-0.09	
484.	F5	11.86	0.67	-0.11	
485.	F2	12.13	0.65	-0.11	
486.	F0	10.93	0.59	-0.07	
487.	F0	12.64	0.62	-0.27	
488.	A4	9.32	0.67	0.03	BD +32°3183
489.	F5	11.49	0.77	-0.21	
490.	F5	11.45	0.87	-0.29	
491.	F4	11.13	0.70	-0.32	BD +32°3170
492.	F4	11.67	0.78	-0.23	
493.	F7	9.4	-	-	BD +32°3175, blend
494.	F4	10.68	0.56	-0.11	
495.	F5	11.61	0.64	-0.19	
496.	F6	10.98	0.79	0.05	
497.	B8	10.03	-0.02	-0.39	BD +32°3165
498.	A8	9.45	0.34	0.02	BD +32°3162
499.	A9	9.35	0.43	0.01	BD +32°3161
500.	A3	9.77	0.27	0.00	BD +32°3159

Table
/Continued/

No.	Sp.	V	B-V	U-B	remarks
501.	F4	12.02	0.52	-0.31	
502.	A2	12.08	0.29	-0.06	
503.	F6	9.96	0.77	-0.11	
504.	F3	9.62	0.46	-0.11	BD $+32^{o}3157$
505.	F5	11.35	0.58	-0.17	
506.	F4	11.89	0.49	-0.18	
507.	F6	10.29	0.58	-0.14	BD $+32^{o}3154$
508.	F2	11.14	0.30	-0.12	
509.	F3	11.12	0.16	-0.03	
510.	F6	10.51	0.55	-0.06	BD $+31^{o}3301$
511.	F6	9.37	0.54	-0.05	BD $+31^{o}3305$
512.	A8	12.37	0.51	-0.11	
513.	A1	9.51	0.01	-0.08	BD $+32^{o}3164$
514.	F6	10.81	0.55	0.03	
515.	A4	12.62	0.30	-0.18	
516.	A8	12.32	0.53	-0.20	
517.	A8	12.47	0.48	-0.07	
518.	F5	10.49	0.54	-0.10	
519.	A6	12.03	0.72	-0.27	
520.	F5	10.38	0.47	-0.07	BD $+31^{o}3310$
521.	F3	10.65	0.38	-0.03	BD $+31^{o}3312$
522.	A5	8.94	0.32	0.07	BD $+31^{o}3311$
523.	A3	13.03	0.54	-0.13	
524.	F6	10.10	0.45	-0.03	

Notes to the table:

An asterisk at the left upper side of the running number denotes photoelectrically measured colours.

Blend is remarked if the photographic image of the measured star is distorted by a neighbouring star.